



Adsorption studies on brilliant green dye in aqueous solutions using activated carbon derived from guava seeds by chemical activation with phosphoric acid

R. Mansour^a, Mohamed Gamal Simeda^{b,*}, A. Zaatout^c

^aBasic Sciences and Engineering Department, Higher Institute of Engineering and Technology, Postal code: 34517, New Damietta, Egypt, Tel. +201008539761; email: drramadanelkatep@yahoo.com (R. Mansour)

^bChemical Engineering Department, Higher Institute of Engineering and Technology, Postal code: 34511, New Damietta, Egypt, Tel. +201018823502; email: eng.modysmsm@gmail.com (M.G. Simeda)

^cChemical Engineering Department, Faculty of Engineering, Alexandria University, Postal code: 21544, Alexandria, Egypt, Tel. +201223379925; email: draazaatout@yahoo.com (A. Zaatout)

Received 10 January 2020; Accepted 21 May 2020

ABSTRACT

In this research, brilliant green dye (BG) has been removed from synthetic wastewater using activated carbon derived from guava seeds (AGSC) which was collected as a waste product from factories producing juice concentrates. A single-stage batch adsorber was designed for adsorption of BG by AGSC based on some experimental parameters such as contact time (5–40 min), adsorbent mass (0.01–0.08 g), temperature (25°C–95°C), pH (3–10), and initial dye concentration (10–100 ppm). The maximum adsorption capacity of AGSC was found to be 80.5 mg/g using the Langmuir isotherm model which is the best-fitted model for the process. The experimental data were fitted well with the pseudo-second-order kinetic model. The changes in functional groups, surface morphology, and chemical composition of AGSC before and after adsorption were identified by Fourier transform infrared spectroscopy, scanning electron microscope, energy-dispersive X-ray spectroscopy, respectively. The specific surface area of AGSC was measured to be 605.1 m²/g using Brunauer–Emmett–Teller analysis. Pore volume and pore diameter were found to be 0.57 cm³/g and 3.78 nm, respectively. The thermodynamic study proved that adsorption of BG on AGSC was physiosorptive ($\Delta G = -7.7$ kJ/mol) and spontaneous at high temperature ($\Delta H = 13.4$ kJ/mol, $\Delta S = 0.07$ kJ/mol K).

Keywords: Brilliant green dye; Activated carbon; Wastewater treatment; Guava seeds

1. Introduction

Coloring agents and dyestuffs become the main feedstock for the production of domestic goods, colorful fabrics, paints, printing inks, and so on. Releasing such toxic dyes from these industries has made a worldwide worry because of their enormous toxicity toward humankind. For instance, the total consumption of dyes by the textile industry, in particular, is in excess of 10⁷ kg/y worldwide with approximately 10⁶ kg/y of discharged dyes into water streams [1]. There are several types of synthetic dyestuffs

that can be found in wastewater and it can be classified into three main classes: anionic (direct, acid, and reactive dyes), cationic (basic dyes), and non-ionic (disperse dyes and vat dyes) [2] while in general, cationic dyes have the most harmful and toxic effects on the ecosystem of receiving water and the whole environment [3]. Many dyes and pigments have cancer-causing and mutagenic impacts that influence oceanic biota by preventing light from penetration through water levels which slow down photosynthetic activity and also tend to toxify fish and other organisms due to chelating metal ions. Oxidation and reduction of these dyes in

* Corresponding author.

water can also produce hazardous substances that raise the necessity of getting rid of them from wastewater [4,5]. For that reason, a number of physical, chemical, and biological methods are in use to separate dyes from wastewater before discharging into water streams [5].

Adsorption has been observed to be better than multiple techniques for wastewater treatment because it is inexpensive, very flexible, modest in design, easy to operate, and does not produce hazardous materials [5]. Commercial activated carbon is a commonly utilized adsorbent in wastewater treatment processes as it consists of a micro-porous homogenous structure that gives large surface area and has no radiation effects but its wide utilization was restricted because it is costly. Hence, scientific researchers have focused their attention on producing activated carbon from renewable domestic agricultural waste because of its low preparation costs [6]. Table 1 shows some previous works in the preparation of activated carbons from agricultural wastes with its specific areas and the name of the adsorbate.

Physical and chemical activation are the basic processes for producing activated carbon. The first technique composed of raw material carbonization and gasification of the resulting char by steam or carbon dioxide. The second technique consists of impregnation of the precursor material with chemical reagent (KOH, $ZnCl_2$, H_2SO_4 , H_3PO_4 , HNO_3 , and CO_2) then carbonization of the impregnated product [16]. $ZnCl_2$ and H_3PO_4 appear to be the most used activating agents for the preparation of activated carbon for wastewater treatment but H_3PO_4 is preferred because of its ease removing after carbon activation by washing with hot or cold water in addition to other environmental and operational features [17]. Moreover, the iodine number for the activated carbon prepared from H_3PO_4 is higher than the iodine number of activated carbon prepared from $ZnCl_2$ [18]. Generally, the chemical activation process has been found to be superior to the physical activation process because the chemical reagents increase the productivity and the surface area of the resulted product [5] and it has lower energy cost than physical because it takes place at a lower temperature and a shorter time [19].

Brilliant Green (BG) is an odorless cationic dye in the form of golden-green crystals [1]. It is known as Diamond green G, Solid green, Ethyl green, and Basic green 1. It can

be used for several purposes such as biological mark, dermatological agent, veterinary medicine, and inhibition of mold propagation in poultry food [20]. It is also widely utilized in the dyeing of textiles and manufacturing of inks for printing papers. About 0.8–1.0 kg of BG is utilized per ton of paper produced [21]. For mankind, BG causes discomfort in the gastrointestinal tract which results in nausea, vomiting, and diarrhea. It also causes harassment in the respiratory tract with cough and shortness of breath. Moreover, it can cause skin irritation with redness and ache in case of direct contact [22]. Decomposition of BG may produce hazardous gases like carbon oxides, nitrogen oxides, and sulfur oxides, the molecular structure of the dye is given in Fig. 1 [2]. As a result, many researchers studied the adsorption of BG from wastewater by some carbonized materials as given in Table 2.

Guava seeds can be considered a waste product after processing of guava juice (fresh guava fruit has 5% seeds from its weight). It contains an abundant amount of lignocellulosic materials which make it desirable for the production of activated carbons [29]. It is used by many researchers to remove some hazardous substances as shown in Table 3.

The current survey was aimed to study this process as a function of time, adsorbent mass, temperature, pH, and initial dye concentration. Some adsorption isotherm models were studied to know the maximum adsorption capacity for the activated guava seeds carbon and the best-fitted model for the process. The kinetic and thermodynamic studies were analyzed to define the mechanism and the rate-controlling stage for the process. The experimental data have been modeled as single-stage batch adsorber using Langmuir isotherm.

2. Materials and methods

2.1. Preparation of the adsorbent

The raw guava seeds were collected from a juice processing factory in New Damietta, Egypt. The raw material was rinsed with boiled water for several times until free from any guava residue. The raw material was dried in an electric oven at 110°C until constant weight then crushed to a very fine powder using a lab scale ball mill. The raw guava powder was placed in a glass container and a concentrated phosphoric acid (85%), a high phosphoric acid concentration

Table 1
Previous studies in the preparation of activated carbon from agricultural wastes

Type of wastes	Specific surface area (m ² /g)	Name of the adsorbate	Reference
Pistachio wood	1,884	Lead(II)	[7]
Sugarcane bagasse	1,113	Carbon dioxide	[8]
Date stones	248	Methylene blue dye	[9]
Coffee shell	2,349	Water vapor	[10]
Pine cone	10	Tetrabromobisphenol	[11]
Peanut shell	1,138	Reactive brilliant blue dye	[12]
Brazilian nutshells	1,651	Basic blue 26 dye	[13]
Açaí stones	990		
Mangosteen peel	1,621	Methylene blue dye	[14]
Coconut husk	1,448	Fluoride	[15]

Table 2
Reported adsorption capacities (Q_m) of BG by different adsorbents

Adsorbent	Maximum adsorption capacity (mg/g)	Reference
Chemically activated Brazilian pine-fruit shell carbon	219.1	[23]
Chemically and physically activated Brazilian pine-fruit shell carbon	263.4	[23]
Chemically activated jute sticks carbon	480	[24]
Steam activated jute sticks carbon	182	[24]
Activated acorn carbon	2.11	[25]
Chemically activated coconut shell carbon	0.008	[26]
Chemically activated corn cob carbon	0.008	[26]
Chemically activated eucalyptus tree carbon	0.007	[26]
Chemically activated flamboyant pod carbon	0.009	[26]
Palm fronds activated carbon	45.45	[27]
Mesoporous activated carbon	826	[28]
Chemically activated guava seeds carbon	80.45	Present work

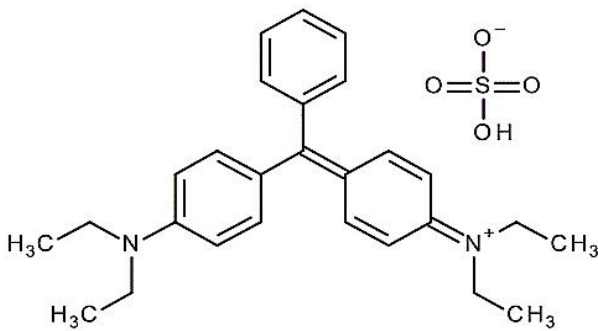


Fig. 1. Molecular structure of the brilliant green dye.

gives high specific surface area and high pore volume for the resulted carbon [36], was poured carefully into the container until 20 g of seeds will be impregnated in 40 mL of H_3PO_4 at 25°C for 24 h. At the end of the soaking time, the soaked seeds were dried in an electric oven at 110°C for 1 h. The seeds were placed on a ceramic cup and subjected to

400°C for 2 h in a muffle furnace (Hobersal JB-20) which contains an exhaust filter that purifies the emitted gases before being discharged into the air. Then, seeds were washed with distilled hot water until the pH was reached 6.5–7, and then the produced activated carbon was dried in an electric oven at 110°C for 3 h in order to remove any undesired moisture within the particles. Finally, the activated guava seeds carbon was sieved using (SAMA Sieve Shaker) to obtain an equal particle diameter which was (75 μ m).

2.2. Preparation of the adsorbate

Brilliant Green dye (Merck, Germany) was bought from the market with molecular weight 482.62 g/mol and was used by dissolving 1 g of BG powder, weighed by a four-digit analytical balance (KERN-ABS 220-4, UK), in 1 L of distilled water to prepare the stock solution (1,000 ppm). The desired experimental concentrations were prepared accordingly by diluting the stock solution with distilled water. The maximum wavelength was found to be 625 nm [3] and the final concentrations were determined using UV-visible spectrophotometer (PG instrument Ltd T80, UK).

Table 3
Previous studies in the preparation of activated carbon from guava seeds

Activation method	Activating agent	Activation conditions		Name of the adsorbate	Reference
		Temperature, °C	Time, min		
Physical activation	Not used	400–600	30–45	Methylene blue dye	[29]
Physical activation	Not used	1,000	240	Acid orange 7 dye	[30]
Physical activation	Not used	600–1,000	240	Acid blue 80, Acid blue 324, Acid green 25, Acid green 27, Acid orange 8, Acid orange 10, and Acid red 1 dyes	[31]
Physical activation	Not used	800	120	Lead	[32]
Chemical activation	ZnCl ₂	700	60	Nickel(II)	[33]
Chemical activation	NaOH	750	90	Amoxicillin	[34]
Chemical activation	ZnCl ₂	500	120	Chlorinated phenol	[35]

2.3. Adsorbent characterization technique

Nitrogen adsorption/desorption measurements were performed at 77 K using the high-speed gas sorption analyzer (NOVA 1000, version 6.11, Quanta Chrome Corporation) employing the Brunauer–Emmett–Teller (BET) method to determine the specific surface area of AGSC. About 0.3 g of AGSC sample is outgassed at 250°C for 2 h before being analyzed to ensure the accuracy of the results. A scanning electron microscopy (SEM, JEOL JSM 6510 Iv, Japan) was used to obtain surface morphology and qualitative elemental composition of AGSC before and after adsorption. A Fourier transform infrared spectrophotometer (FTIR, ThermoFisher Nicolette IS10, USA) was used to clarify the chemical changes in the surface of AGSC before and after adsorption.

2.4. Adsorption studies

Batch adsorption process was carried out to study the effect of experimental parameters (contact time, adsorbent mass, temperature, pH, and initial dye concentration) on the adsorption of BG by AGSC. Firstly, a constant weight of the adsorbent (0.02 g) was allowed to contact with a 50 mL of a BG solution at different concentrations (10–50 ppm) at neutral pH in a 125 mL glass bottles at a fixed temperature (25°C ± 2°C) and shaking speed (240 rpm) in a shaking water bath (Wisd laboratory instruments, DAHAN Scientific Co., Ltd., 30, Korea) for a time period between 5 and 40 min until it reached the equilibrium (30 min). Secondly, the solutions were centrifuged using (80-1 electric centrifuge) and the concentrations of the filtrated samples were determined by the spectrophotometer.

In order to investigate the effect of adsorbent mass, the previous procedures were applied at (0.01–0.08 g) of AGSC and constant time (30 min) until the equilibrium was observed at 0.06 g. The effect of temperature was studied by applying the above procedures at 30 min contact time, 0.06 g adsorbent mass, neutral pH, and different temperatures (25°C–95°C). The initial dye concentration effect was determined by preparing (10–100 ppm) from the stock of the dye solution and applying the repeated process at the optimized conditions of the previous parameters (30 min, 0.06 g). The pH parameter was investigated at pH range (3–10) of the dye solutions using a pH-meter (Hanna-Instruments 8519, pH 211, Canada), (0.1 N) HCl, and (0.1 N) NaOH and repeating the process as described above at equilibrium time and adsorbent mass until it gives the highest removal percent at pH = 9.

The process efficiency was calculated according to the following equations:

$$(\%R) = \left[1 - \left(\frac{C_e}{C_0} \right) \right] \times 100 \tag{1}$$

$$Q_e = \frac{(C_0 - C_e)V}{W} \tag{2}$$

where “ C_0 ” is the initial concentration of BG solution in ppm, “ C_e ” is the final concentration of BG solution in ppm, “ V ” is the volume of BG solution in L, and “ W ” is the mass

of the adsorbent in g. “ Q_e ” is the adsorption capacity at equilibrium (mg/g).

3. Results and discussion

3.1. Characterization of AGSC

3.1.1. BET analysis

The specific surface area was measured to be 605.1 m²/g and by assuming a uniform cylindrical pore, so the total amount of nitrogen taken up at a pressure of 1 atm and a temperature of 77 K gives the total pore volume [37] which is 370.3326 cm³/g as shown in Fig. 2 and after converting it to the liquid volume it will be 0.57 cm³/g and the pore diameter will be 3.78 nm using Wheeler Equation as follows:

$$D_p = 4,000 \times \frac{V_p}{S_{BET}} \tag{3}$$

where “ D_p ” is the average pore diameter in nm, “ V_p ” is the total pore volume in cm³/g, and “ S_{BET} ” is the specific surface area in m²/g [37].

3.1.2. SEM analysis

Fig. 3a displays a heterogeneous morphology of AGSC before adsorption of BG including many small pores that are distributed randomly on the surface. Fig. 3b clearly shows the aggregation of BG particles on the surface of AGSC which makes the pores mostly disappeared and this indicates that BG was successfully adsorbed on the surface of AGSC.

3.1.3. EDXS analysis

Table 4 illustrates the differences in weight percent between AGSC loaded and unloaded with BG where it can be seen that the weight percent of oxygen increased after adsorption which may be interpreted that oxygen atoms were adsorbed on the surface of AGSC as the dye contains four atoms of oxygen (C₂₇H₃₄N₂O₄S) while the weight percent of carbon and phosphorus decreased which may be interpreted that they reacted with the dye molecules and formed other compounds. So, it can be concluded that

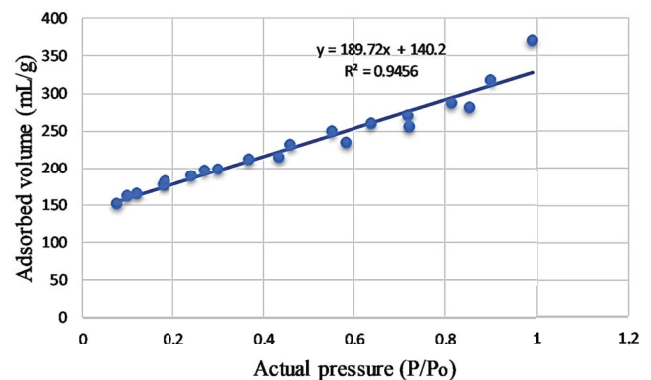


Fig. 2. BET isotherm data for AGSC.

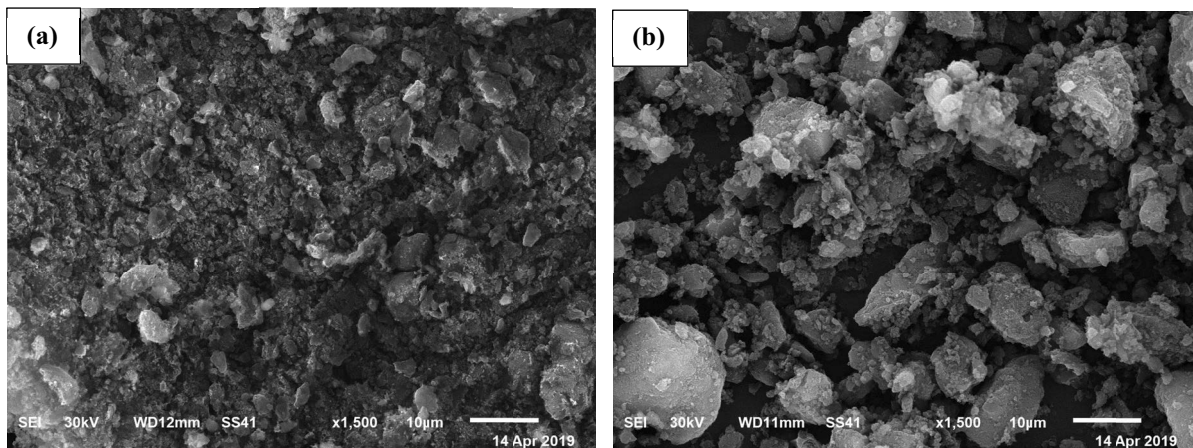


Fig. 3. Scanning electron microscopy of (a) AGSC (b) before and after adsorption of BG.

Table 4
EDXS analysis of AGSC before and after adsorption of BG

Elements	Wt.% before	Wt.% after
C	79.92	79.79
O	18.45	18.77
P	1.03	0.88
Cu	0.37	0.34
Zn	0.23	0.22

the chemical structure of AGSC was changed due to the effective adsorption of BG molecules on the pores of AGSC.

3.1.4. FTIR analysis

Fig. 4 presents the difference in the IR spectrum of AGSC before and after adsorption of BG. According to AGSC before adsorption of BG, there are some strong and moderately strong bands at 3,430; 2,854; 1,591; 1,441; 1,378;

1,163; 1,071; 574, and 471 cm^{-1} assigned to O–H stretch [38,39,41], Methylene C–H symmetric stretch [38–41], primary amine N–H bend [38–41], methyl C–H asymmetric bend [38–41], methyl C–H symmetric bend [38–41], tertiary alcohol C–O stretch [38–41], C–O–C cyclic ethers [38,39,41], C–S stretch disulfides [38], and S–S stretch polysulfides [38]. On the other hand, AGSC after adsorption of BG has strong, moderate and weak bands at 3,432; 2,853; 2,052; 1,657; 1,581; 1,438; 1,380; 1,338; 1,217; 1,181; 1,153; 1,069; and 886 cm^{-1} assigned to O–H stretch [38,39,41], methylene C–H symmetric stretch [38–41], phenyl isothiocyanate –N=C=S [38,41], primary amide C=O stretch [38–41], secondary amine N–H bend [38,39,41], methyl C–H asymmetric bend [38,40,41], methyl C–H symmetric bend [38–41], methyne C–H bend [38,39,40], P–O–C aromatic phosphates stretch [38,40,41], R–O– SO_3^- organic sulfates [38,39,41], tertiary alcohol C–O stretch [38–41], C–O–C cyclic ethers [38,39,41], cyclic acid anhydrides C–C stretch [39,40].

The observed shifts of the bands in the IR spectrum to higher and lower wavelength as well as the appearance of new bands at 2,052; 1,657; 1,338; 1,217; 1,181; and 886 cm^{-1}

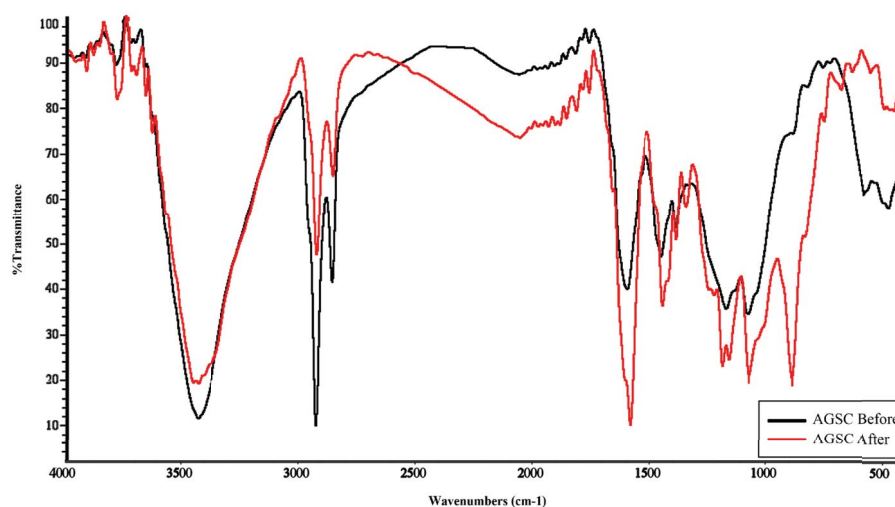


Fig. 4. Fourier transform infrared spectroscopy of AGSC before and after adsorption of BG.

and disappearance of some bands at 574 and 471 cm^{-1} can be considered strong evidence for the adsorption of BG on the surface of AGSC.

3.2. Effect of operating conditions

3.2.1. Contact time

Fig. 5 represents the effect of contact time for the adsorption of different concentrations (10–50 ppm) of BG onto a fixed weight (0.02 g) of AGSC in the range of 5–40 min. It can be observed that the low concentrations (10, 20, and 30 ppm) reach the equilibrium very rapidly at the first 10 min while the high concentrations (40 and 50 ppm) reach the equilibrium at (30 min) after a gradual increase in the removal percent during the time period shown in the figure and this could be interpreted by the theory that in adsorption of dyes, firstly, the dye molecules have to compete against the effect of boundary layer interface. Secondly, the penetrating dye molecules move out from the boundary layer film to distribute onto the surface of the adsorbent. Finally, the remaining dye molecules diffuse into the porous structure of the adsorbent. Based on this theory, we conclude that when the initial concentration of dye solutions increases, the amount of dye molecules increases, so the process will take relatively longer contact time to reach the equilibrium state [3].

3.2.2. The adsorbent mass

As shown in Fig. 6, the removal percent of 10–50 ppm BG onto AGSC increases with the increase in adsorbent mass ranged from 0.01 to 0.06 g due to the availability of more adsorbent active sites as well as greater availability of specific surface area of the adsorbent. After that there are no significant changes in removal percent were observed because of overlapping or aggregation of adsorption sites results in a decrease in total adsorbent surface area available

to BG and an increase in diffusion path length, and this leads to a slighter increase in BG removal [42]. So, 0.06 g can be considered the optimal mass for AGSC loading.

3.2.3. Temperature of the process

Temperature has a significant effect on the adsorption process because it can affect the diffusion rate of dye molecules at the external boundary layer interface, and also inside the adsorbent pores [5]. Fig. 7 displays the temperature influence for adsorption of BG at 10–50 ppm on the surface of AGSC with constant weight (0.06 g). It is clearly shown that as temperature increased in the range 25°C–95°C, the removal percent of BG increased from 96% to 99%. Because increasing temperature will decrease the viscosity of the dye solution which increases the diffusion rate of dye molecules across the external boundary layer and in the internal pores of the adsorbent particle and also may increase the tendency of disaggregation and so the uptake of the BG particles [43].

3.2.4. Initial dye concentration

This parameter was studied in the range 10–100 ppm at temperature 25°C, 0.06 g adsorbent mass, and 30 min contact time. From Fig. 8, it was observed that the removal percent decreased slightly with the increase in initial concentration up to 60 ppm then it decreased sharply with the increase in initial concentration from 60 to 90 ppm, and after 90 ppm it was clearly noticed that there were no considerable changes in the removal percent and this can be explained by the fact that at low initial dye concentration the number of active sites on the adsorbent's surface is more available compared to high initial dye concentration. So, most of the dye molecules have been adsorbed on the surface of AGSC at low initial BG concentration leading to higher percentage removal while at high initial BG

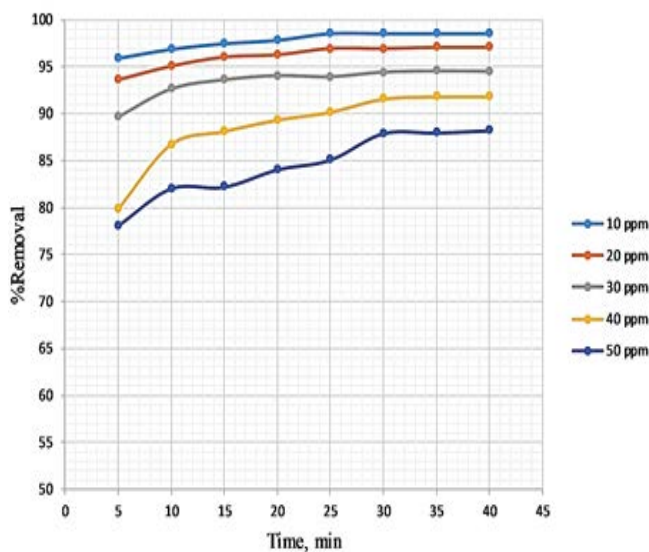


Fig. 5. Effect of contact time on the adsorption of BG dye onto AGSC.

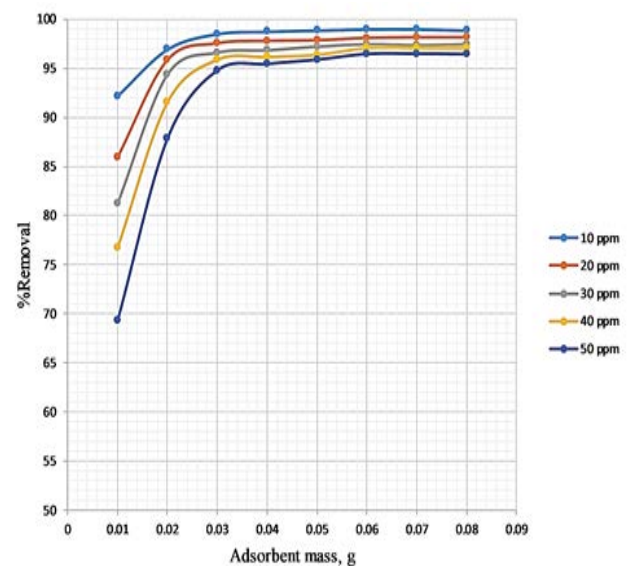


Fig. 6. Effect of adsorbent mass on the adsorption of BG dye onto AGSC.

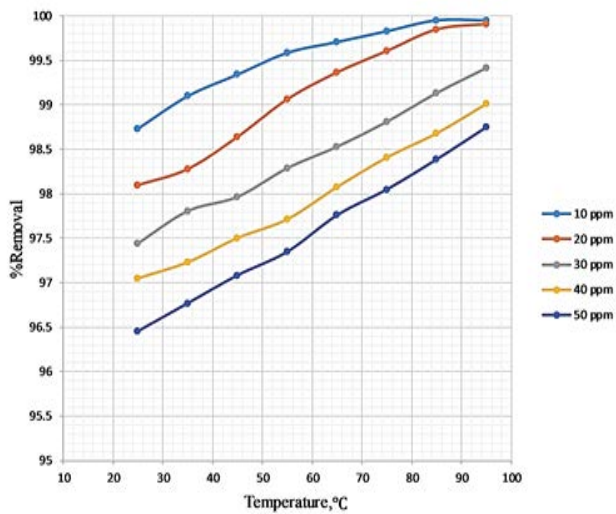


Fig. 7. Effect of temperature on the adsorption of BG dye onto AGSC.

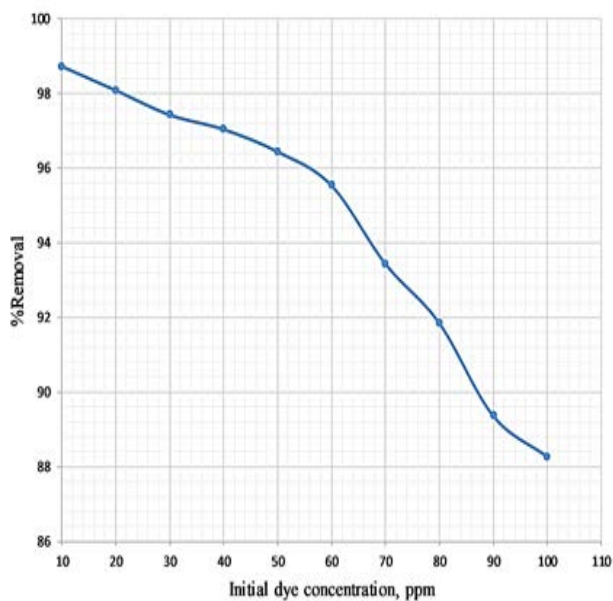


Fig. 8. Effect of initial dye concentration on the adsorption of BG dye onto AGSC.

concentration, molecules have low chances to be adsorbed due to the limited number of binding sites at the adsorbent's surface. Thus, some of the dye molecules remain in the solution and do not get adsorbed [3].

3.2.5. pH of the process

The pH parameter was investigated within the range 3–10 at 10–50 ppm initial concentration of BG as shown in Fig. 9. The results indicate that the removal percent of BG increases with the increase in pH up to 9 after which was observed no significant improvement in the process. The maximum removal percent was 99%.

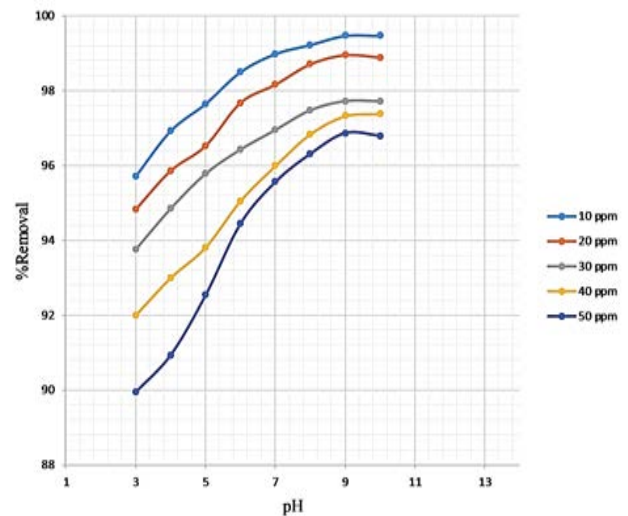


Fig. 9. Effect pH on the adsorption of BG dye onto AGSC.

The surface charge of AGSC may get positively charged at lower pH which makes H^+ ions compete effectively with dye cation leading to a decrease in the removal percent of dye adsorbed while at higher pH, the surface of AGSC may get negatively charged which enhances the electrostatic force of attraction between the positively charged dye cation and the adsorbent's surface [44].

3.3. Isotherm and equilibrium study

The isotherm study was carried out by fitting the experimental data to four isotherm models and find a convenient model that can be used for design purposes using the correlation coefficients, R^2 values as shown in Table 5 and Fig. 10.

For Langmuir model, C_e/Q_e vs. C_e has a linear relationship as shown in Fig. 10a, with a slope equal to $1/Q_m$ and an intercept equal to $1/(Q_m K_L)$. The linear Langmuir equation is given as:

$$\frac{C_e}{Q_e} = \frac{1}{(Q_m K_L)} + \frac{C_e}{Q_m} \quad (4)$$

where " Q_m " is the maximum adsorption capacity (mg/g), and " K_L " is the Langmuir affinity constant (L/mg) related to " Q_m " and rate of adsorption. The feasibility of the process can be evaluated by a separation factor (dimensionless constant) " R_L " which is given in the following equation:

$$R_L = \frac{1}{(1 + (K_L C_0))} \quad (5)$$

The " R_L " value lays between zero and one for favorable adsorption, whereas $R_L > 1$, $R_L = 1$, and $R_L = 0$ for unfavorable, linear, and irreversible adsorption, respectively [45,46].

For Freundlich model, $\ln Q_e$ vs. C_e has a linear relationship as shown in Fig. 10b, with an intercept equal to $\ln K_f$ and a slope equal to $1/n$.

Table 5
Adsorption isotherm of BG dye on AGSC at 298 K

Isotherm models	Parameter value	Isotherm models	Parameter value
Langmuir		Temkin	
Q_m (mg/g) [45,46]	80.45329	K_t (L/mg) [46]	9.035467
K_L (L/mg) [45,46]	0.589695	q_m (J/mol) [45,46]	14.90977
R_L	0.144992	R^2	0.979
R^2	0.9922		
Freundlich		Dubinin-Radushkevich	
K_f (mg/g) [45,46]	26.24116	Q_m (mg/g) [45,46]	49.87887
$1/n$	0.470575	D (mol ² /J ²) [46]	0.069032
R^2	0.9703	R^2	0.8205

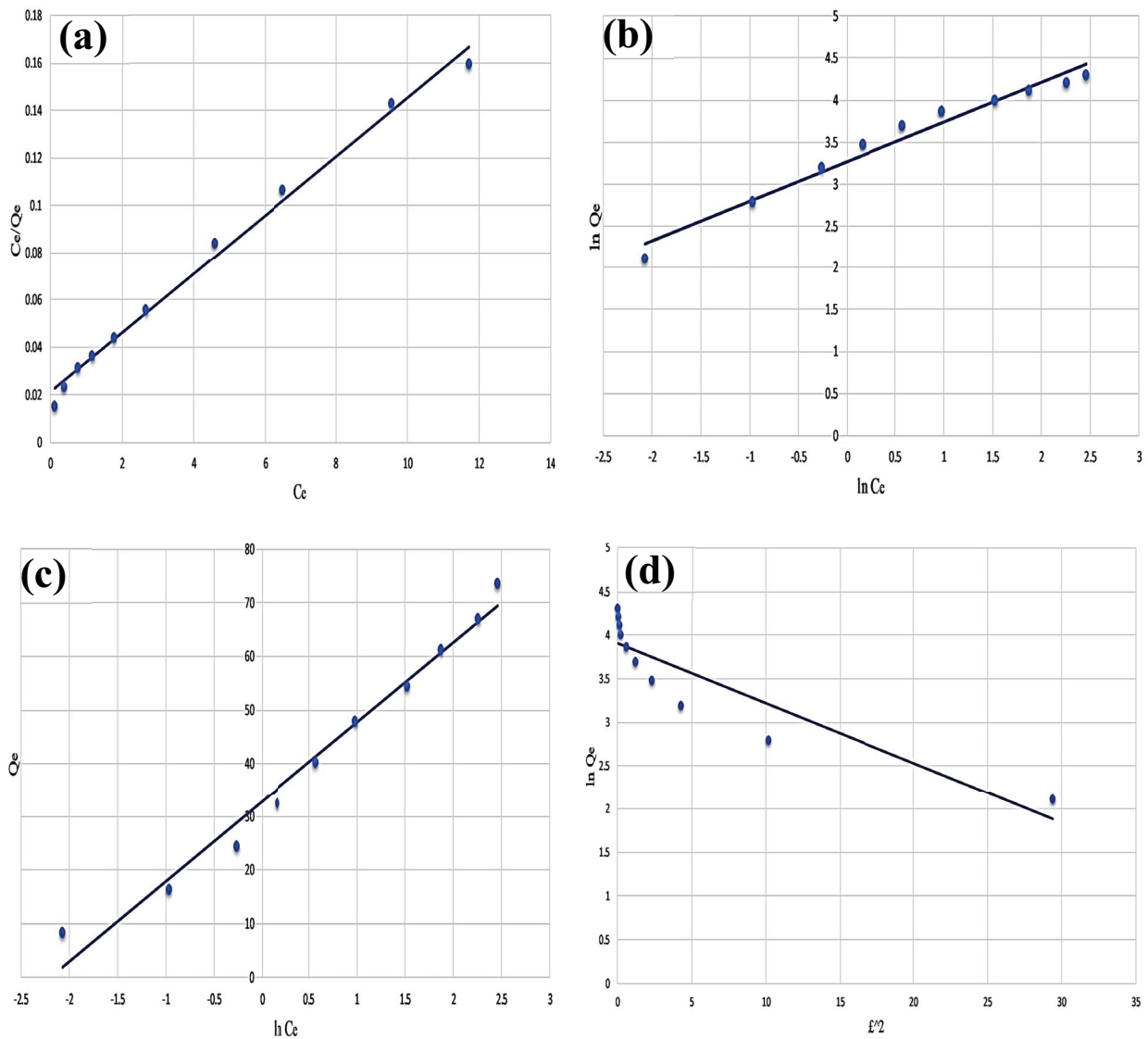


Fig. 10. Adsorption isotherm models of BG dye on AGSC (a) Langmuir model, (b) Freundlich model, (c) Temkin model, and (d) Dubinin–Radushkevich model.

The logarithmic form of Freundlich is given by the following equation:

$$\ln Q_e = \left(\frac{1}{n}\right) \ln C_e + \ln K_f \quad (6)$$

where “ K_f ” is the Freundlich constant which represents the adsorption capacity of the adsorbent in mg/g and $1/n$ gives an indication for the favorability of the adsorption process. If the value of $1/n$ lay between 0 and 1 it means adequate adsorption [45,46].

The Temkin model's equation can be expressed as:

$$Q_e = q_m \ln K_t + q_m \ln C_e \quad (7)$$

where K_t and q_m are Temkin constants related to adsorption capacity in L/mg and heat of sorption in J/mol, respectively [45,46]. The values of q_m and K_t can be obtained from the slope and intercept of the linear plot of Q_e vs. $\ln C_e$ as displayed in Fig. 10c.

The Dubinin–Radushkevich model can be represented by the following equations:

$$\ln Q_e = \ln Q_m - D\varepsilon^2 \quad (8)$$

$$\varepsilon = RT \ln \left(\frac{C_e + 1}{C_e} \right) \quad (9)$$

where ε is Polanyi potential, R is the ideal gas constant (8.314 J/mol K), T is the absolute temperature in K, and D , Q_m are Dubinin constants related to the transfer of adsorption energy in mol²/J² and the maximum adsorption capacity of the adsorbent in mg/g, respectively. The Dubinin constants can be calculated from the slope and intercept of the plot between $\ln Q_e$ and ε^2 in Fig. 10d [46].

3.4. Kinetic study

Four kinetic models were used to fit the experimental data at 50 ppm initial dye concentration using a linear regression analysis method as given in Fig. 11 and the parameters of these models are summarized in Table 6.

The pseudo-first-order rate expression is given as:

$$\log(Q_e - Q_t) = \log(Q_e) - \left(\frac{K_1 \cdot t}{2.303} \right) \quad (10)$$

where Q_t is the amount of dye adsorbed on the adsorbent at any time, t in mg/g, and K_1 is the first-order rate constant. A Fig. 11a of $\log(Q_e - Q_t)$ vs. t gives a linear relationship from which the value of K_1 and Q_e can be determined from the slope and intercept [47].

The linearized form of the pseudo-second-order model is given as:

$$\frac{t}{Q_t} = \left(\frac{1}{K_2 \cdot Q_e^2} \right) + \frac{t}{Q_e} \quad (11)$$

where K_2 is the rate constant of the pseudo-second-order adsorption. The plot of t/Q_t vs. t in Fig. 11b gives a linear relationship from which Q_e and K_2 can be determined from the slope and intercept of the plot, respectively [48].

The Elovich model is generally expressed as:

$$Q_t = \left(\frac{1}{(\beta \cdot \ln[\alpha \cdot \beta])} \right) + \left(\frac{1}{(\beta \cdot \ln[t])} \right) \quad (12)$$

where α is the initial adsorption rate (mg/g min) and β is related to the extent of surface coverage and the activation energy for chemisorption (g/mg) [48]. A plot of Q_t vs. $\ln t$ in Fig. 11c gives a linear relationship with a slope of $1/\beta$ and an intercept of $1/\beta \ln(\alpha\beta)$.

The intra-particle diffusion model used here refers to the theory proposed by Weber and Morris based on the following equation:

$$Q_t = K_{pi} \cdot t^{0.5} + C \quad (13)$$

where K_{pi} (mg/g min^{0.5}) is the intra-particle diffusion rate constant and C (mg/g) describes the boundary layer thickness [3]. The plot of Q_t vs. $t^{0.5}$ in Fig. 11d gives a linear relationship of slope (K_{pi}) and an intercept (C).

3.5. Thermodynamic study

The thermodynamic parameters that used to describe the adsorption process are the change of Gibbs free energy (ΔG° , kJ/mol), enthalpy (ΔH° , kJ/mol), and entropy (ΔS° , kJ/mol/K). They are calculated depending on the equilibrium experimental data obtained at different temperatures from 298.15 to 338.18 K and at 50 ppm initial dye concentration by using the Van't Hoff equations as follow:

$$\Delta G = -RT \ln K \quad (14)$$

$$\ln K = \frac{\Delta S}{R} - \left(\frac{\Delta H}{R \cdot T} \right) \quad (15)$$

where R is the ideal gas constant (8.314 J/mol/K), T is the absolute temperature in kelvin, and $K = Q_e/C_e$.

The enthalpy (ΔH°) and entropy (ΔS°) of the process were estimated from the slope and intercept of the plot of $\ln K$ vs. $1/T$ as shown in Fig. 12. Table 7 shows that ΔG° values are negative at all temperatures so, adsorption of BG onto AGSC is a physiosorptive and spontaneous process because the free energy values fall in the range of -20 to 0 kJ/mol [3]. Hence, the links between dye molecules and the adsorbent surface can be due to Van deer-Waals or electrostatic attraction forces [45]. The positive values of ΔH° and ΔS° indicate that the adsorption of BG onto AGSC is an endothermic reaction and the increase in temperature facilitates dye adsorption by displacing water molecules from AGSC's surface [3].

3.6. Design of single-stage batch adsorber

The design of batch adsorber is considered the practicable step for equilibrium data resulted from experimental

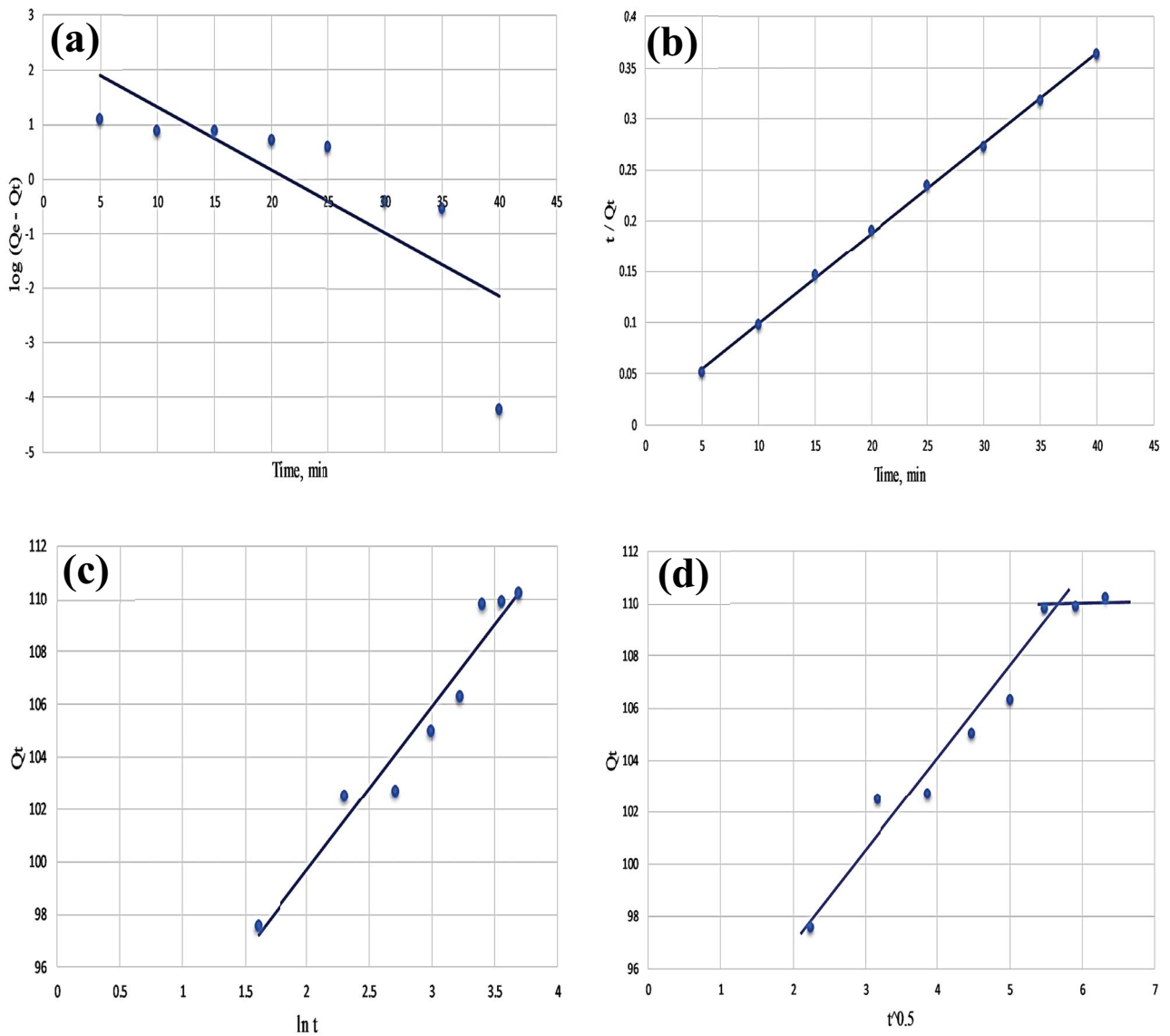


Fig. 11. Kinetic models of BG dye adsorption on AGSC (a) pseudo-first-order, (b) pseudo-second-order, (c) Elovich, and (d) intra-particle diffusion.

Table 6
Kinetics study of BG dye on AGSC

Kinetic models	Value	Kinetic models	Value
Pseudo-first-order		Elovich	
Q_e "experimental" (mg/g)	110.2119	α (mg/g min)	7538744
Q_e "calculated" (mg/g)	293.2076	β (g/mg)	0.160584
K_1 (1/min)	0.265163	R^2	0.9514
R^2	0.6368		
Pseudo-second-order		Intra-particle diffusion	
Q_e "experimental" (mg/g)	110.2119	K_{pi} (mg/g min ^{0.5})	3.128541
Q_e "calculated" (mg/g)	113.139	C (mg/g)	91.24119
K_2 (g/mg min)	0.007431	R^2	0.9583
R^2	0.9993		

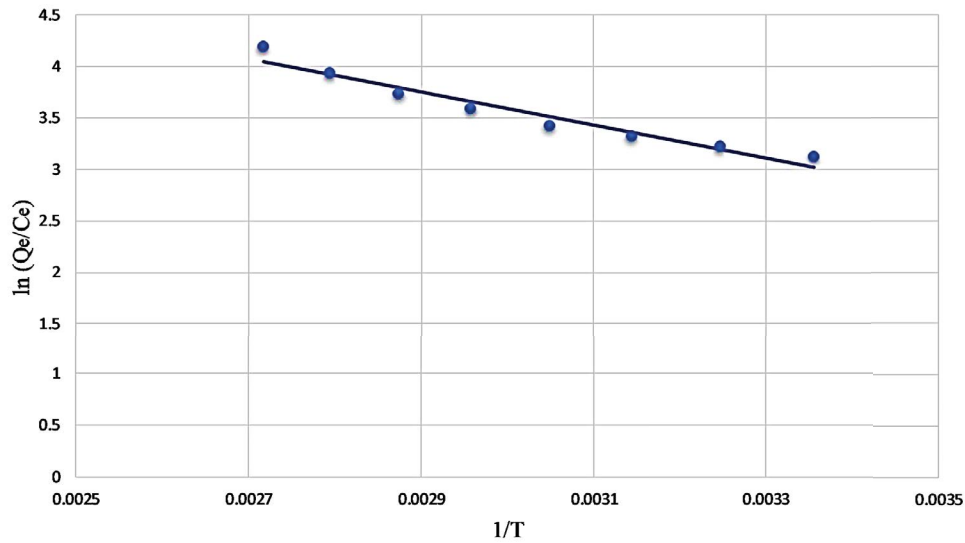


Fig. 12. Graphical determination of ΔH° and ΔS° .

Table 7
Thermodynamic parameters of BG dye onto AGSC

Temperature (K)	ΔG° (kJ/mol)	ΔH° (kJ/mol)	ΔS° (kJ/mol K)
298.15	-7.7319	13.394047	0.0700689
308.15	-8.2378		
318.15	-8.7849		
328.15	-9.3298		
338.15	-10.101		
348.15	-10.811		
358.15	-11.701		
368.15	-12.822		

work by calculating the required adsorber volume and the optimum adsorbent weight [45]. Fig. 13 displays a schematic diagram for single-stage batch adsorber where the initial concentration of the dye changes from C_0 to C_e and the adsorption capacity of the adsorbent changes from Q_0 to Q_e .

The mass balance for the batch adsorber with a solution volume (V) and the amount of adsorbent (M) can be written as follow:

$$M \cdot Q_0 + V \cdot C_0 = M \cdot Q_e + V \cdot C_e \quad (16)$$

$$V(C_0 - C_e) = M(Q_e - Q_0) \quad (17)$$

By using the Langmuir adsorption isotherm model as it is the best-fitted model and by assuming that AGSC is a fresh adsorbent ($Q_0 = 0$) so, Eq. (17) can be rearranged as follow:

$$\frac{M}{V} = \frac{(C_0 - C_e)}{Q_e} = \frac{(C_0 - C_e)}{[(Q_m \cdot K_L \cdot C_e) / (1 + (K_L \cdot C_e))]} \quad (18)$$

Based on the previous equation, a relationship was drawn in Fig. 14a between the mass of adsorbent and the volume of dye solution that needs to be treated (100:2,000 L) at a removal percent equal to 85% and a range of initial dye concentration from 20 to 100 ppm.

Otherwise, a relationship was drawn in Fig. 14b between the previous variables but at different removal percent (60%:98%) and constant initial dye concentration (200 ppm).

3.7. Proposed mechanism for the process

The general methodology for any adsorption process can be summarized in the following stages:

- The dye molecules have to encounter the boundary layer effect for the adsorbent and diffuse from the boundary layer film onto the adsorbent surface.
- Diffusion of the dye molecules into the porous structure of the adsorbent where intra-particle diffusion of solute takes place in the adsorbed state or in the liquid-filled pores of the particle.

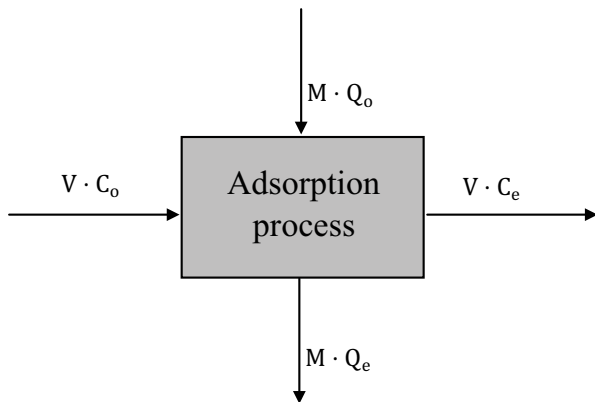


Fig. 13. Single-stage batch adsorber unit.

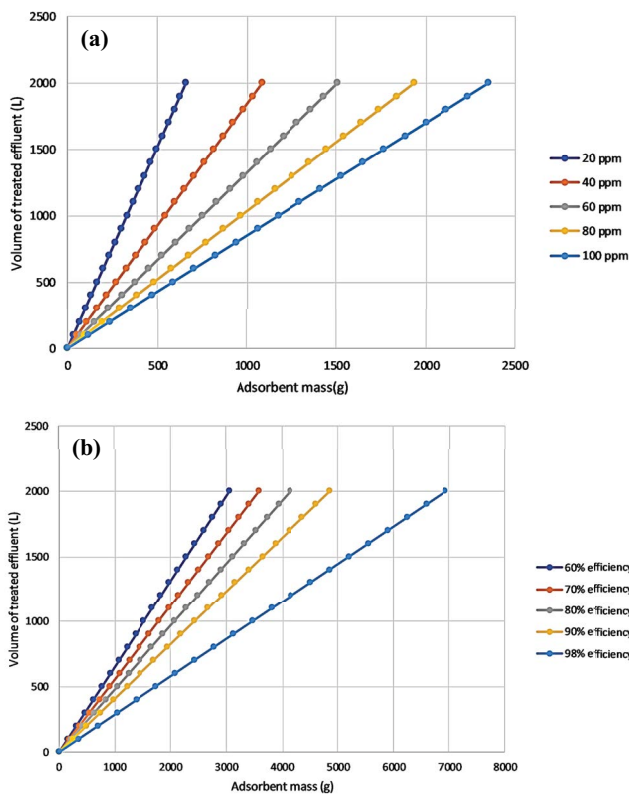


Fig. 14. Relation between the mass of the adsorbent and volume of the dye solution (a) at 85% efficiency and (20:100 ppm) initial dye concentration and (b) at 200 ppm initial dye concentration and efficiency from 60% to 98%.

In the case of a well-stirred batch adsorber, the first stage occurs speedily due to reducing the boundary layer with continuous stirring so, the second stage is likely to be the rate-controlling stage [3,45].

According to the kinetic study, the pseudo-second-order model is the best-fitted model for this process ($R^2 > 0.99$) and from Fig. 11d it's clearly observed that the plot doesn't pass through the origin. Therefore, it can be concluded that the second stage is the rate-controlling stage [3,45].

According to FTIR analysis displayed in Fig. 4, it's clearly shown that OH groups which act as active adsorption sites on the surface of AGSC have a decrease in its peak intensity due to forming hydrogen bonds with BG molecules [45] and this could be confirmed by the negative values of ΔG° in the thermodynamic study which falls in the range of -20 to 0 kJ/mol [3].

According to the thermodynamic study, the positive value of entropy is a strong indication of replacing the water molecules in the pores of AGSC with BG molecules by increasing temperature which makes the first stage occurs very rapidly [3].

Therefore, the process methodology can be deduced as follows:

- BG molecules encounter the boundary layer film and diffused rapidly onto the surface of AGSC due to continuous shaking and heating of bottles by the shaking water bath (Wisd laboratory instruments, DAHAN Scientific Co., Ltd., 30, Korea).
- Intra-particle diffusion of BG molecules takes place in the porous structure of AGSC where hydrogen bonds (Van der-Waals or electrostatic attraction forces) were formed between BG molecules and the hydroxyl groups on the surface of AGSC until the process reaches the equilibrium state.

4. Conclusion

This study showed that activated carbon prepared from guava seeds by chemical activation with phosphoric acid was a favorable adsorbent for the removal of brilliant green dye from aqueous solutions over a wide range of concentrations. The optimum experimental data were 30 min contact time, 0.06 g adsorbent mass, and basic medium pH = 9. Kinetic and equilibrium studies were best fitted with the pseudo-second-order kinetic model ($R^2 > 0.99$) and Langmuir isotherm model ($R^2 > 0.99$) where the maximum adsorption capacity was found to be 80.5 mg/g. The negative values of ΔG° were demonstrated that the process is physical adsorption and spontaneous at high temperatures with respect to the positive values of ΔH° and ΔS° which proved that the reaction is endothermic and as the temperature increase, the separation of water molecules from the adsorbent surface increase so, the efficiency of the process increase. Pore volume and pore diameter were found to be 0.57 cm³/g and 3.78 nm, respectively by assuming a uniform cylindrical pore. A single-stage batch adsorber was designed based on the Langmuir model to remove 20–100 ppm initial dye concentration with 85% efficiency and 200 ppm initial dye concentration with 60%–98% efficiency.

References

- [1] V.S. Mane, P.V.V. Babu, Studies on the adsorption of Brilliant green dye from aqueous solution onto low-cost NaOH treated saw dust, *Desalination*, 273 (2011) 321–329.
- [2] K.B. Tan, M. Vakili, B.A. Horri, P.E. Poh, A.Z. Abdullah, B. Salamatinia, Adsorption of dyes by nanomaterials: recent developments and adsorption mechanisms, *Sep. Purif. Technol.*, 150 (2015) 229–242.
- [3] M. Saif Ur Rehman, M. Munir, M. Ashfaq, N. Rashid, M.F. Nazar, M. Danish, J.I. Han, Adsorption of Brilliant Green

- dye from aqueous solution onto red clay, *Chem. Eng. J.*, 228 (2013) 54–62.
- [4] J. Gao, Q. Zhang, K. Su, R. Chen, Y. Peng, Biosorption of Acid yellow 17 from aqueous solution by non-living aerobic granular sludge, *J. Hazard. Mater.*, 174 (2010) 215–225.
 - [5] H. Amor, A. Mabrouk, N. Talmoudi, Preparation of activated carbon from date stones: optimization on removal of indigo carmine from aqueous solution using a two-level full factorial design, *Int. J. Eng. Res. Gen. Sci.*, 3 (2015) 6–17.
 - [6] M.B. Alqaragully, Removal of textile dyes (Maxilon blue, and Methyl orange) by date stones activated carbon, *Int. J. Adv. Res. Chem. Sci.*, 1 (2014) 48–59.
 - [7] S.A. Sajjadi, A. Meknati, E.C. Lima, G.L. Dotto, D.I. Mendoza-Castillo, I. Anastopoulos, F. Alakhras, E.I. Unuabonah, P. Singh, A. Hosseini-Bandegharai, A novel route for preparation of chemically activated carbon from pistachio wood for highly efficient Pb(II) sorption, *J. Environ. Manage.*, 236 (2019) 34–44.
 - [8] J. Han, L. Zhang, B. Zhao, L. Qin, Y. Wang, F. Xing, The N-doped activated carbon derived from sugarcane bagasse for CO₂ adsorption, *Ind. Crops Prod.*, 128 (2019) 290–297.
 - [9] G. Abdelali, C. Abdelmalek, Y.A. Réda, S. Ammar, N. Boubekeur, Removal of methylene blue using activated carbon prepared from date stones activated with NaOH, *Global Nest J.*, 21 (2019) 374–380.
 - [10] S. Sun, Q. Yu, M. Li, H. Zhao, C. Wu, Preparation of coffee-shell activated carbon and its application for water vapor adsorption, *Renewable Energy*, 142 (2019) 11–19.
 - [11] J. Shen, G. Huang, C. An, X. Xin, C. Huang, S. Rosendahl, Removal of tetrabromobisphenol A by adsorption on pinecone-derived activated charcoals: synchrotron FTIR, kinetics and surface functionality analyses, *Bioresour. Technol.*, 247 (2018) 812–820.
 - [12] H. Wu, R. Chen, H. Du, J. Zhang, L. Shi, Y. Qin, L. Yue, J. Wang, Synthesis of activated carbon from peanut shell as dye adsorbents for wastewater treatment, *Adsorpt. Sci. Technol.*, 37 (2019) 34–48.
 - [13] T. Nayara, V. De Souza, M. Gurgel, A. Vieira, M. Gurgel, H₃PO₄-activated carbons produced from açai stones and Brazil nut shells: removal of basic blue 26 dye from aqueous solutions by adsorption, *Environ. Sci. Pollut. Res.*, 26 (2019) 28533–28547.
 - [14] A. Nasrullah, B. Saad, A.H. Bhat, A.S. Khan, M. Danish, M.H. Isa, A. Naeem, Mangosteen peel waste as a sustainable precursor for high surface area mesoporous activated carbon: characterization and application for methylene blue removal, *J. Cleaner Prod.*, 211 (2019) 1190–1200.
 - [15] K. Singh, S.H. Hasan, O. Nath, Effective removal of fluoride from water by coconut husk activated carbon in fixed bed column: experimental and breakthrough curves analysis, *Groundwater Sustainable Dev.*, 7 (2018) 48–55.
 - [16] T. Ahmad, M. Danish, M. Rafatullah, A. Ghazali, O. Sulaiman, R. Hashim, M.N.M. Ibrahim, The use of date palm as a potential adsorbent for wastewater treatment: a review, *Environ. Sci. Pollut. Res.*, 19 (2012) 1464–1484.
 - [17] M.d.R. Moreno-Virgen, R. Tovar-Gómez, D.I. Mendoza-Castillo, A. Bonilla-Petriciolet, Applications of Activated Carbons Obtained from Lignocellulosic Materials for the Wastewater Treatment, V.H. Montoya, Ed., *Lignocellulosic Precursors Used in the Synthesis of Activated Carbon – Characterization Techniques and Applications in the Wastewater Treatment*, BoD–Books on Demand, México, 2012. pp. 58–71.
 - [18] F. Al-Qaessi, L. Abu-Farah, Activated carbon production from date stones using phosphoric acid, *Energy Sources Part A*, 32 (2010) 1316–1325.
 - [19] K. Mahmoudi, N. Hamdi, E. Srasra, Preparation and characterization of activated carbon from date pits chemical activation with zinc chloride for methyl orange adsorption, *J. Mater. Environ. Sci.*, 5 (2014) 1758–1769.
 - [20] B.K. Nandi, A. Goswami, M.K. Purkait, Adsorption characteristics of brilliant green dye on kaolin, *J. Hazard. Mater.*, 161 (2009) 387–395.
 - [21] V.S. Mane, I. Deo Mall, V. Chandra Srivastava, Kinetic and equilibrium isotherm studies for the adsorptive removal of Brilliant Green dye from aqueous solution by rice husk ash, *J. Environ. Manage.*, 84 (2007) 390–400.
 - [22] A. Mittal, D. Kaur, J. Mittal, Applicability of waste materials-bottom ash and deoiled soya-as adsorbents for the removal and recovery of a hazardous dye, brilliant green, *J. Colloid Interface Sci.*, 326 (2008) 8–17.
 - [23] T. Calvete, E.C. Lima, N.F. Cardoso, S.L.P. Dias, E.S. Ribeiro, Removal of brilliant green dye from aqueous solutions using home made activated carbons, *Clean Soil Air Water*, 38 (2010) 521–532.
 - [24] M. Asadullah, M. Asaduzzaman, M.S. Kabir, M.G. Mostofa, T. Miyazawa, Chemical and structural evaluation of activated carbon prepared from jute sticks for Brilliant Green dye removal from aqueous solution, *J. Hazard. Mater.*, 174 (2010) 437–443.
 - [25] M. Ghaedi, H. Hossainian, M. Montazerzohori, A. Shokrollahi, F. Shojaiipour, M. Soylak, M.K. Purkait, A novel acorn based adsorbent for the removal of brilliant green, *Desalination*, 281 (2011) 226–233.
 - [26] A.F. Ali, A.S. Kovo, S.A. Adetunji, Methylene blue and brilliant green dyes removal from aqueous solution using agricultural wastes activated carbon, *J. Encapsulation Adsorpt. Sci.*, 7 (2017) 95–107.
 - [27] A.F. Ahmad, G.A. Elchaghaby, Palm fronds activated carbon for the removal of brilliant green dye from wastewater, *Water Desal. Res. J.*, 2 (2018) 1–10.
 - [28] A. Aichour, H. Zaghouane-Boudiaf, Highly brilliant green removal from wastewater by mesoporous adsorbents: kinetics, thermodynamics and equilibrium isotherm studies, *Microchem. J.*, 146 (2019) 1255–1262.
 - [29] K. Soon, Sorption studies of methylene blue in aqueous solution by optimized carbon prepared from guava seeds (*Psidium guajaval*), *Mater. Sci.*, 13 (2007) 83–87.
 - [30] M.P. Elizalde-González, V. Hernández-Montoya, Removal of acid orange 7 by guava seed carbon: a four parameter optimization study, *J. Hazard. Mater.*, 168 (2009) 515–522.
 - [31] M.P. Elizalde-González, V. Hernández-Montoya, Guava seed as an adsorbent and as a precursor of carbon for the adsorption of acid dyes, *Bioresour. Technol.*, 100 (2009) 2111–2117.
 - [32] L. Largette, T. Brudey, T. Tant, P.C. Dumesnil, P. Lodewyckx, Comparison of the adsorption of lead by activated carbons from three lignocellulosic precursors, *Microporous Mesoporous Mater.*, 219 (2016) 265–275.
 - [33] T.M. Zewail, S.A.M. El-Garf, Preparation of agriculture residue based adsorbents for heavy metal removal, *Desal. Water Treat.*, 22 (2010) 363–370.
 - [34] O. Pezoti, A.L. Cazetta, K.C. Bedin, L.S. Souza, C. Martins, T.L. Silva, O.O.S. Júnior, J.V. Visentainer, C. Vitor, NaOH-activated carbon of high surface area produced from guava seeds as a high-efficiency adsorbent for amoxicillin removal: kinetic, isotherm and thermodynamic studies, *Chem. Eng. J.*, 288 (2015) 778–788.
 - [35] S.M. Anisuzzaman, C.G. Joseph, D. Krishnaiah, A. Bono, E. Suali, S. Abang, L.M. Fai, Removal of chlorinated phenol from aqueous media by guava seed (*Psidium guajava*) tailored activated carbon, *Water Resour. Ind.*, 16 (2016) 29–36.
 - [36] S.M. Yakout, G.S. El-deen, Characterization of activated carbon prepared by phosphoric acid activation of olive stones, *Arabian J. Chem.*, 9 (2016) S1155–S1162.
 - [37] A.C. Martins, O. Pezoti, A.L. Cazetta, K.C. Bedin, D.A.S. Yamazaki, G.F.G. Bandoch, T. Asefa, J.V. Visentainer, V.C. Almeida, Removal of tetracycline by NaOH-activated carbon produced from macadamia nut shells: kinetic and equilibrium studies, *Chem. Eng. J.*, 260 (2015) 291–299.
 - [38] J. Coates, Interpretation of infrared spectra, a practical approach, *Encycl. Anal. Chem.*, (2006) 10815–10837.
 - [39] B.C. Smith, *Infrared Spectral Interpretation: A Systematic Approach*, CRC Press, UK, 1998.
 - [40] A.C.S. Talari, M.A.G. Martinez, Z. Movasaghi, S. Rehman, I.U. Rehman, Advances in Fourier transform infrared (FTIR) spectroscopy of biological tissues, *Appl. Spectrosc. Rev.*, 52 (2017) 456–506.

- [41] P. Larkin, *Infrared and Raman Spectroscopy Principles and Spectral Interpretation*, 1st Ed., Elsevier, Netherlands, 2011.
- [42] H.H. Hammud, A. Shmait, N. Hourani, Removal of malachite green from water using hydrothermally carbonized pine needles, *RSC Adv.*, 5 (2015) 7909–7920.
- [43] S. Karaca, A. Gürses, M. Açıkyıldız, M. Ejder (Korucu), Adsorption of cationic dye from aqueous solutions by activated carbon, *Microporous Mesoporous Mater.*, 115 (2008) 376–382.
- [44] R. Baccar, P. Blázquez, J. Bouzid, M. Feki, M. Sarrà, Equilibrium, thermodynamic and kinetic studies on adsorption of commercial dye by activated carbon derived from olive-waste cakes, *Chem. Eng. J.*, 165 (2010) 457–464.
- [45] R.A. Mansour, N.M. Aboeleneen, N.M. Abdel-Monem, Adsorption of cationic dye from aqueous solutions by date pits: equilibrium, kinetic, thermodynamic studies, and batch adsorber design, *Int. J. Phytorem.*, 20 (2018) 1062–1074.
- [46] R. Kecili, C.M. Hussain, Chapter 4 - Mechanism of Adsorption on Nanomaterials, C.M. Hussain, Ed., *Nanomaterials in Chromatography*, Elsevier Inc., Netherlands, 2018, pp. 89–115.
- [47] D. Pathania, S. Sharma, P. Singh, Removal of methylene blue by adsorption onto activated carbon developed from *Ficus carica* bast, *Arabian J. Chem.*, 10 (2017) S1445–S1451.
- [48] M. Rajabi, O. Moradi, M. Sillanpää, K. Zare, A.M. Asiri, S. Agarwal, V.K. Gupta, Removal of toxic chemical ethidium monoazide bromide using graphene oxide: thermodynamic and kinetics study, *J. Mol. Liq.*, 293 (2019) 1–9, doi: 10.1016/j.molliq.2019.111484.